Theory and simulation of liquid crystal sandwiches

Paulo Teixeira[1,2], Candy Anquetil-Deck[3] and Doug Cleaver[4]

[1]Instituto Superior de Engenharia de Lisboa, Instituto Politécnico de Lisboa, Portugal
[2]Centro de Física Teórica e Computacional,
Faculdade de Ciências da Universidade de Lisboa, Portugal
[3]Department of Chemical Engineering, Norwegian University of Science and Technology,
Trondheim, Norway
[4]Materials and Engineering Research Institute, Sheffield Hallam University, United Kingdom

Background I

- The building blocks of liquid crystals come in a variety of shapes, all non-spherical:

elongated molecules

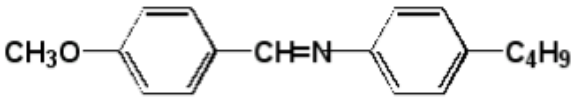

mineral particles

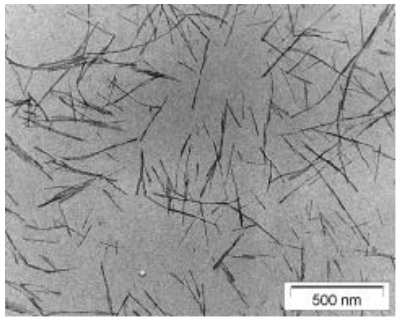

viruses

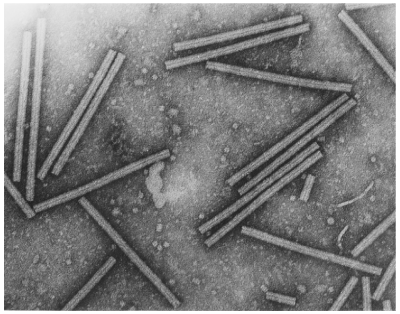

red blood cells

Backgound II

- All current LC devices use confined LCs.

Backgound II

- All current LC devices use confined LCs.
- Their operation relies on the balance between the aligning actions of the bounding surfaces – their anchoring – and of applied fields.

Backgound II

- All current LC devices use confined LCs.
- Their operation relies on the balance between the aligning actions of the bounding surfaces – their anchoring – and of applied fields.
- So the fundamental problem at the heart of LC applications is to understand how given bounding surfaces modify the properties of a given LC to induce a resultant alignment.

Backgound II

- All current LC devices use confined LCs.
- Their operation relies on the balance between the aligning actions of the bounding surfaces – their anchoring – and of applied fields.
- So the fundamental problem at the heart of LC applications is to understand how given bounding surfaces modify the properties of a given LC to induce a resultant alignment.
- Confinement introduces additional structure and new phase transitions. Theories of inhomogeneous fluids are difficult.

Backgound II

- All current LC devices use confined LCs.
- Their operation relies on the balance between the aligning actions of the bounding surfaces – their anchoring – and of applied fields.
- So the fundamental problem at the heart of LC applications is to understand how given bounding surfaces modify the properties of a given LC to induce a resultant alignment.
- Confinement introduces additional structure and new phase transitions. Theories of inhomogeneous fluids are difficult.
- So we seek a simple, generic microscopic model – preferably steric.

Backgound II

- All current LC devices use confined LCs.
- Their operation relies on the balance between the aligning actions of the bounding surfaces – their anchoring – and of applied fields.
- So the fundamental problem at the heart of LC applications is to understand how given bounding surfaces modify the properties of a given LC to induce a resultant alignment.
- Confinement introduces additional structure and new phase transitions. Theories of inhomogeneous fluids are difficult.
- So we seek a simple, generic microscopic model – preferably steric.

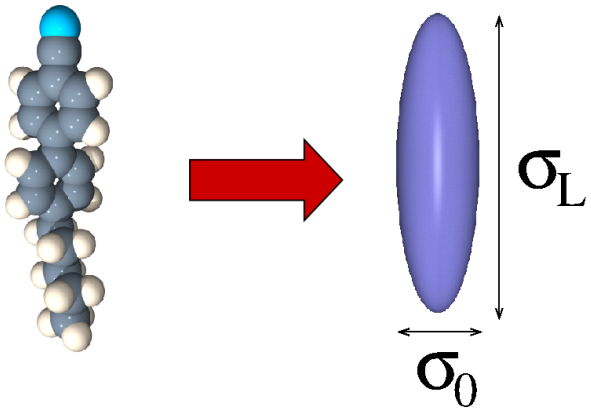

A simple liquid crystal model

- Hard Gaussian overlap (HGO) particles approximate hard ellipsoids

$$U(12) = \begin{cases} 0 & \text{if } r_{12} \geq \sigma(12) \\ \infty & \text{if } r_{12} < \sigma(12) \end{cases}$$

$$\sigma(12) = \sigma_0 \left[1 - \frac{1}{2}\chi \left\{ \frac{(\hat{\mathbf{r}}_{12} \cdot \hat{\omega}_1 + \hat{\mathbf{r}}_{12} \cdot \hat{\omega}_2)^2}{1 + \chi(\hat{\omega}_1 \cdot \hat{\omega}_2)} + \frac{(\hat{\mathbf{r}}_{12} \cdot \hat{\omega}_1 - \hat{\mathbf{r}}_{12} \cdot \hat{\omega}_2)^2}{1 - \chi(\hat{\omega}_1 \cdot \hat{\omega}_2)} \right\} \right]^{-\frac{1}{2}}$$

$$\chi = \frac{\kappa^2 - 1}{\kappa^2 + 1} \quad , \quad \kappa = \frac{\sigma_L}{\sigma_0} \quad \text{particle elongation}$$

- Distance of closest approach given in closed form.
- $\kappa > 1$ prolate (rod-like); $\kappa < 1$: oblate (disc-like).

How to model a confined LC

For prolate (rod-like) particles ($\kappa > 1$), we use the hard needle-wall (HNW) potential:

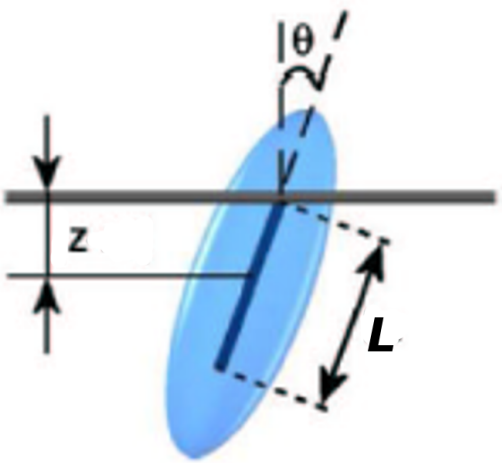

For oblate (disc-like) particles ($\kappa > 1$), we use the hard disc-wall (HDW) potential:

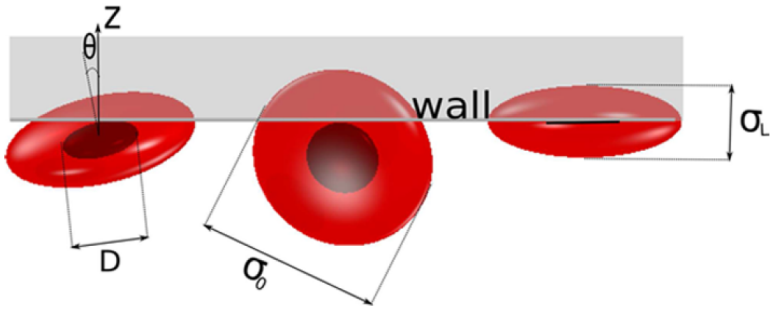

$$\beta\mathcal{V}^{HNW}(z,\theta) = \begin{cases} 0 & \text{if } z \geq \frac{1}{2}L\cos\theta \\ \infty & \text{if } z < \frac{1}{2}L\cos\theta \end{cases} \qquad \beta\mathcal{V}^{HDW}(z,\theta) = \begin{cases} 0 & \text{if } z \geq \frac{1}{2}D\sin\theta \\ \infty & \text{if } z < \frac{1}{2}D\sin\theta \end{cases}$$

Varying L (D) between 0 and $\sigma_L(\sigma_L)$ is equivalent to changing the degree of penetrability of the substrates, e.g., by manipulating the density or the orientation of an adsorbed layer.This can be done independently at either substrate, leading to symmetric or hybrid films.

Theory I

- Write down grand-canonical free energy functional for this system – Onsager second-virial with Parsons-Lee correction to approximate sum of higher-order virial coefficients:

$$\frac{\beta\Omega\left[\rho(z,\omega)\right]}{S_{xy}} = \int \rho(z,\omega)\left[\log\rho(z,\omega) - 1\right]\, dz\, d\omega$$

$$-\frac{F_{HS}^{exc}}{8v_{HS}} \int\int \rho(z_1,\omega_1)\Xi(z_1,\omega_1,z_2,\omega_2)\rho(z_2,\omega_2)\, dz_1 d\omega_1 dz_2 d\omega_2$$

$$+\int \left[\sum_{i=1}^{2} \mathcal{V}^{HDW}(z - z_0^i, \theta) - \mu\right] \rho(z,\omega)\, dz d\omega$$

  where F_{HS}^{exc} is the Carnahan-Starling excess free energy of hard spheres of volume v_{HS}, at the same packing fraction ξ.

- Minimise it to find equilibrium state.

Theory II

- Structure is given by the density profile $\rho(z)$:

$$\rho(z) = \int \rho(z, \omega)\, d\omega$$

- Particle orientations are described by order parameters:

$$\begin{aligned} Q_{zz}(z) &= \langle P_2(\cos\theta) \rangle \qquad \text{(uniaxial)} \\ Q_{xx}(z) - Q_{yy}(z) &= \frac{3}{2} \left\langle \sin^2\theta \, \cos 2\phi \right\rangle \qquad \text{(biaxial)} \\ q(z) &= \left[\frac{2}{3} \operatorname{Tr} \mathbf{Q}^2(z) \right]^{1/2} \qquad \text{(total)} \end{aligned}$$

where $\mathbf{Q}$ is the usual order parameter tensor in the lab-fixed frame:

$$\mathbf{Q} = \begin{bmatrix} Q_{xx} & Q_{xy} & Q_{xz} \\ Q_{yx} & Q_{yy} & Q_{yz} \\ Q_{zx} & Q_{zy} & Q_{zz} \end{bmatrix}$$

Theory III

In fact, the theory gives you lots of orientational order parameters. . . Here is what they all mean.

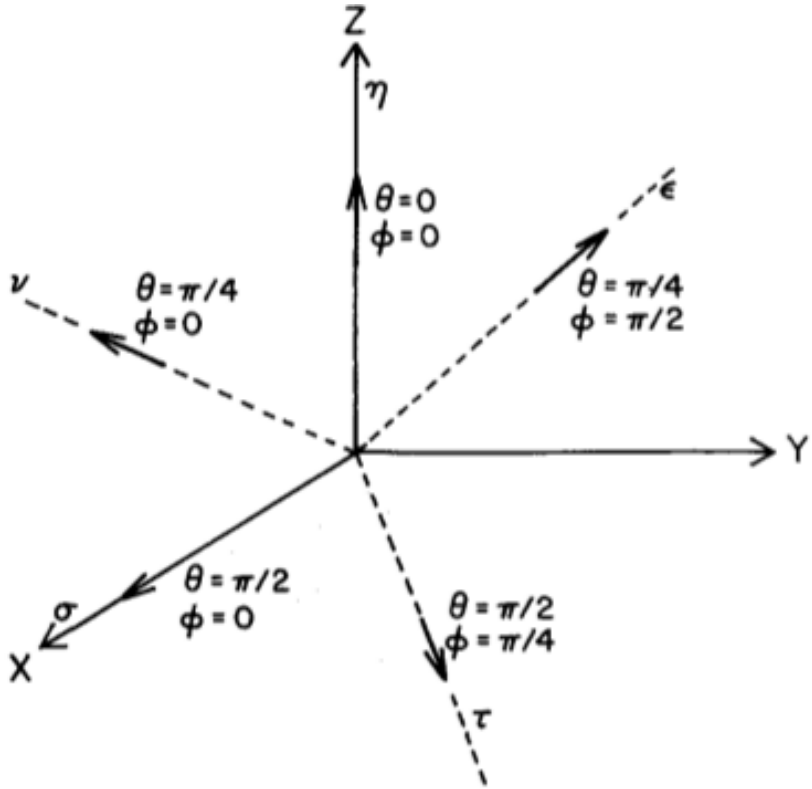

Figure 2. The five second-order orientational order parameters; their equilibrium values give the fraction of molecules aligned in that direction.

M. M. Telo da Gama, Molec. Phys. **52**, 585-610 (1984)

Theory IV

Exactly how do we minimise the free-energy functional?

Theory IV

Exactly how do we minimise the free-energy functional?

- Derive Euler-Lagrange equations, then solve by Picard iteration (traditional, works well).

$$\rho^{(i+1)}(z,\omega) = (1-\alpha)\rho^{(i)}(z,\omega) + \alpha\rho^{(i-1)}(z,\omega) \quad , 0 \leq \alpha < 1$$

Theory IV

Exactly how do we minimise the free-energy functional?

- Derive Euler-Lagrange equations, then solve by Picard iteration (traditional, works well).

$$\rho^{(i+1)}(z,\omega) = (1-\alpha)\rho^{(i)}(z,\omega) + \alpha\rho^{(i-1)}(z,\omega) \quad ,0 \leq \alpha < 1$$

- Direct minimisation using conjugate gradients (didn't work too well).

Theory IV

Exactly how do we minimise the free-energy functional?

- Derive Euler-Lagrange equations, then solve by Picard iteration (traditional, works well).

$$\rho^{(i+1)}(z,\omega) = (1-\alpha)\rho^{(i)}(z,\omega) + \alpha\rho^{(i-1)}(z,\omega) \quad , 0 \leq \alpha < 1$$

- Direct minimisation using conjugate gradients (didn't work too well).
- Artificial neural network (NN) – unsupervised multi-layer perceptron (MLP) (works as well as Picard, sometime better).

Discotic liquid crystals

- Rod-like liquid crystals are well studied. A lot less is known about liquid crystals made up of discs or plates – discotics (DLCs).
- Archetypal discogenic molecules have a rigid aromatic core with 3-, 4- or 6-fold rotational symmetry, and generally 6+ flexible side-chains, each with 5+ atoms.

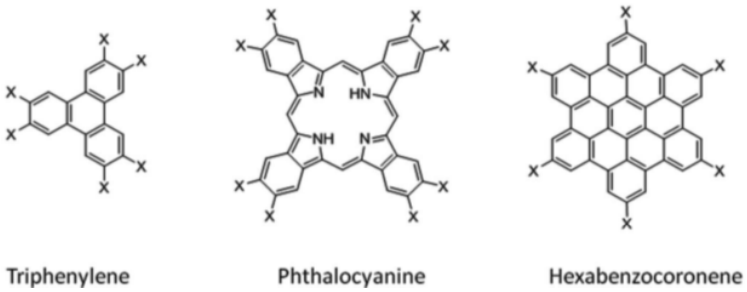

- DLCs have some potentially very interesting and useful applications:
  - Optical compensating films
  - Organic field-effect transistors (OFETs)
  - Organic light-emitting displays (OLEDs)
  - Photovoltaic devices (PVDs) and light-harvesting systems
  - The electronic nose
  - Specialist lubricants
- It makes sense to model them, especially in the confined environments that occur in many technologies.

R. J. Bushby and K. Kawata, Liq. Cryst. **38**, 1415-1426 (2011)

Results: bulk phase diagram

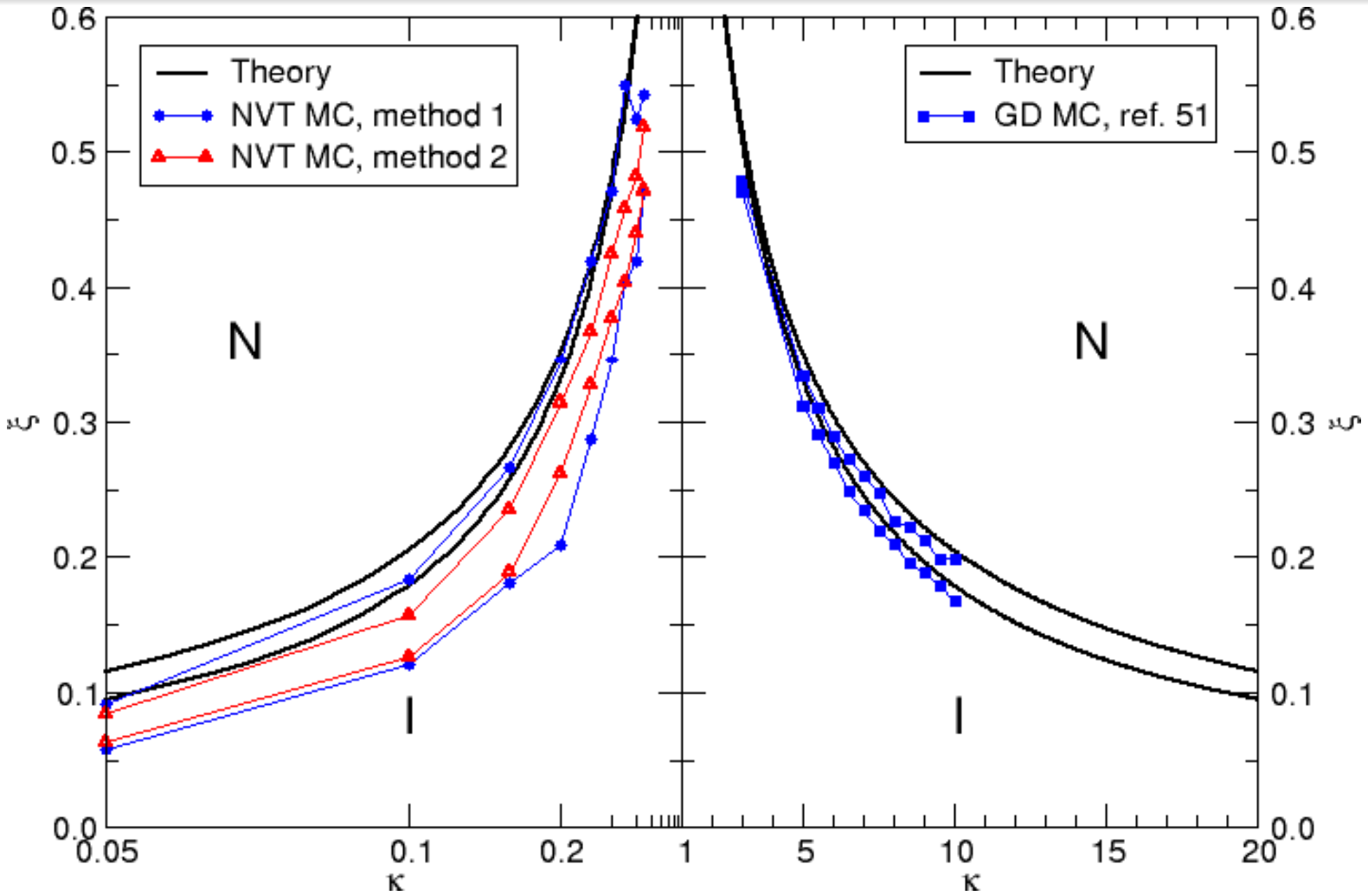

- Better agreement between theory and simulation for prolate particles.
- For oblate particles, density gap at I–N transition independent of elongation.

Results for rods

Simulations

- *NVT* Monte Carlo (MC) of particles of $\kappa = 3$, sandwiched between two substrates a distance L_z apart. Periodic boundary conditions in transverse directions.
- Number of particles is $N = 1000$ for $L_z = 12\sigma_0$, $N = 1250$ for $L_z = 18\sigma_0$, $N = 200$ for $L_z = 24\sigma_0$.
- Each system was compressed from the I phase into the N density range. Typical run lengths at each state point were 5×10^5 MC sweeps (one sweep represents one attempted move per particle) of equilibration, followed by a production run of 5×10^5 sweeps.

Results: density and Q profiles, symmetric film, $L_s = 0$

Bulk density $\rho^* = 0.28$ in I range.

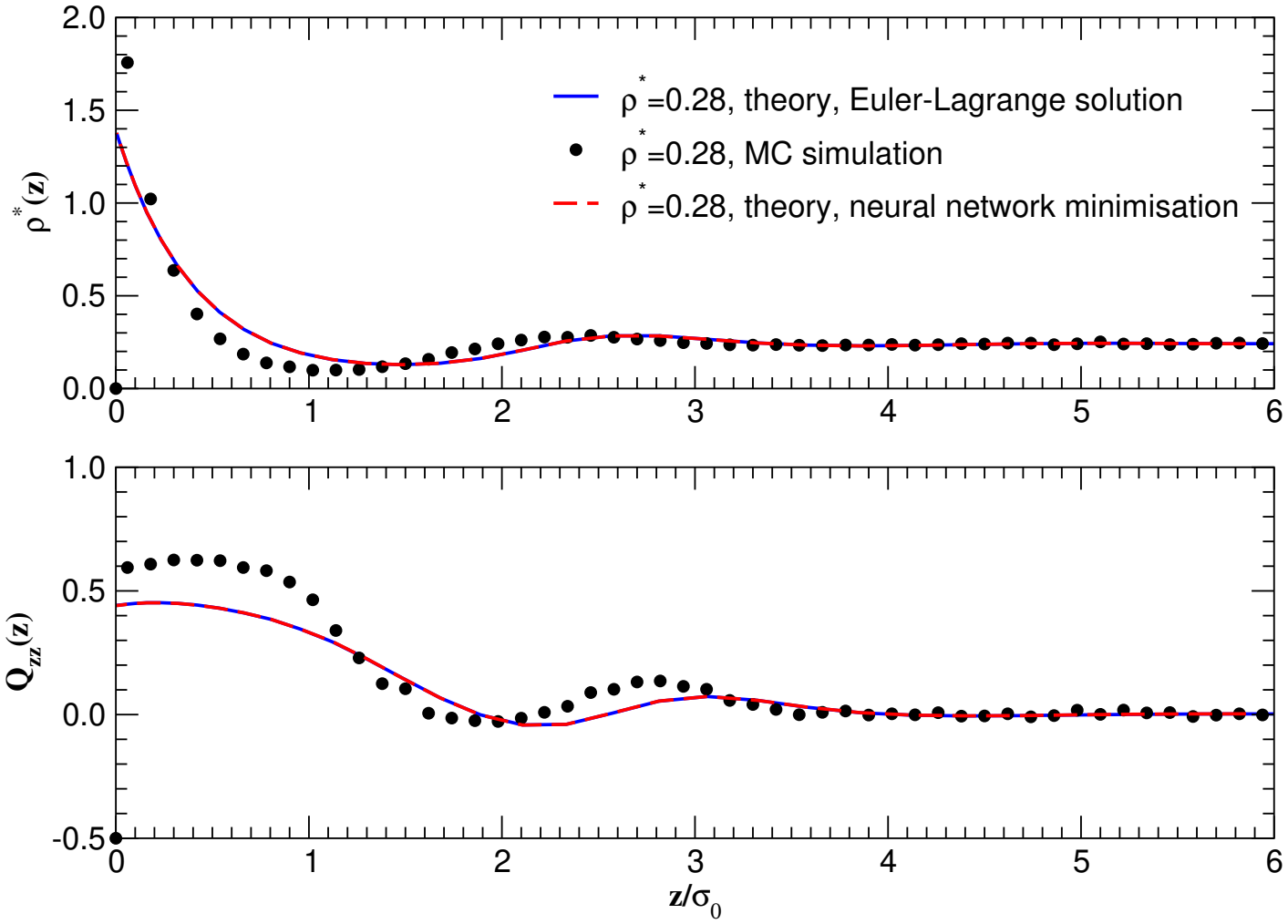

Results: density and Q profiles, symmetric film, $L_s = 0$

Bulk density $\rho^* = 0.35$ in N range.

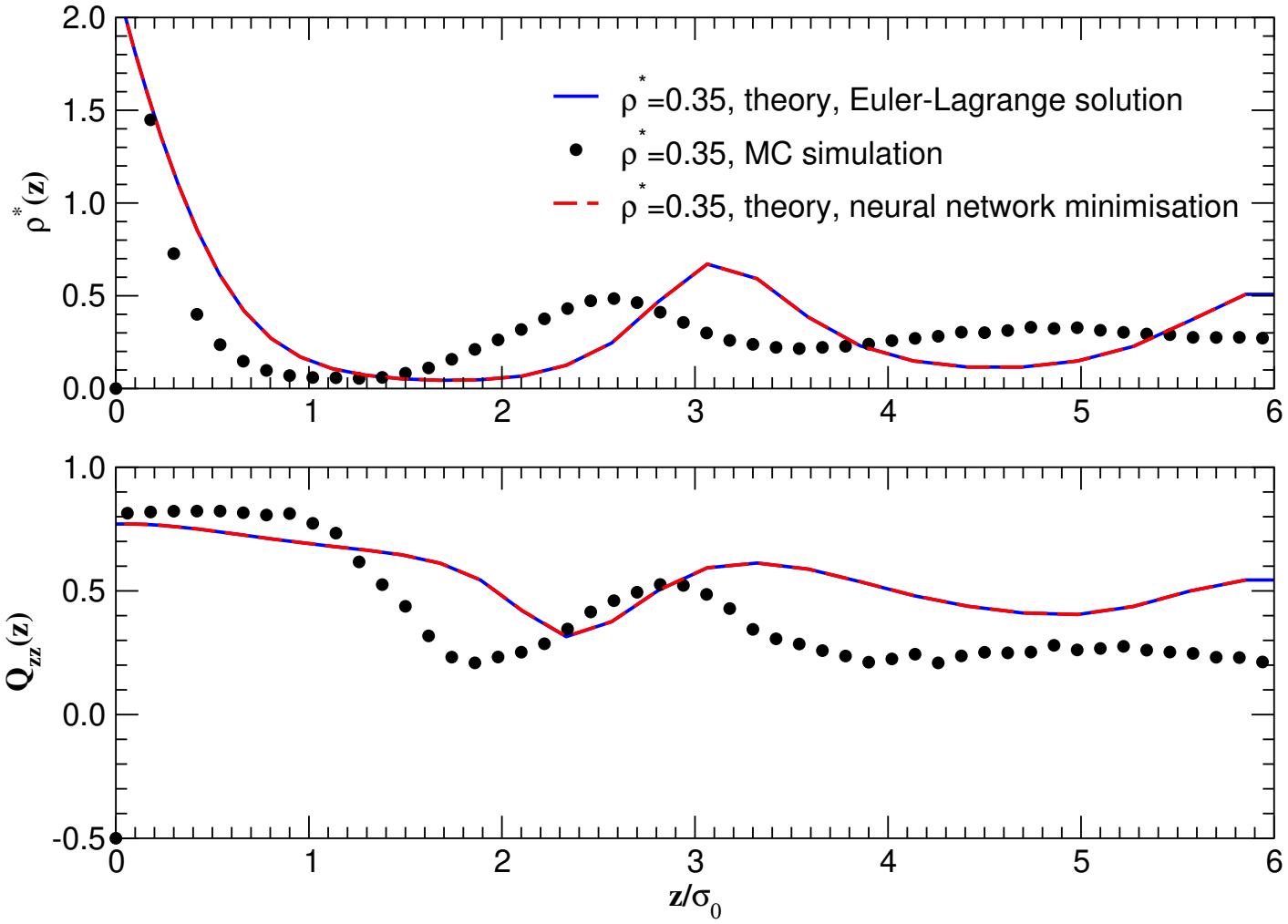

Results: density and Q profiles, symmetric film, $L_s = 2/3$

Bulk density $\rho^* = 0.28$ in I range

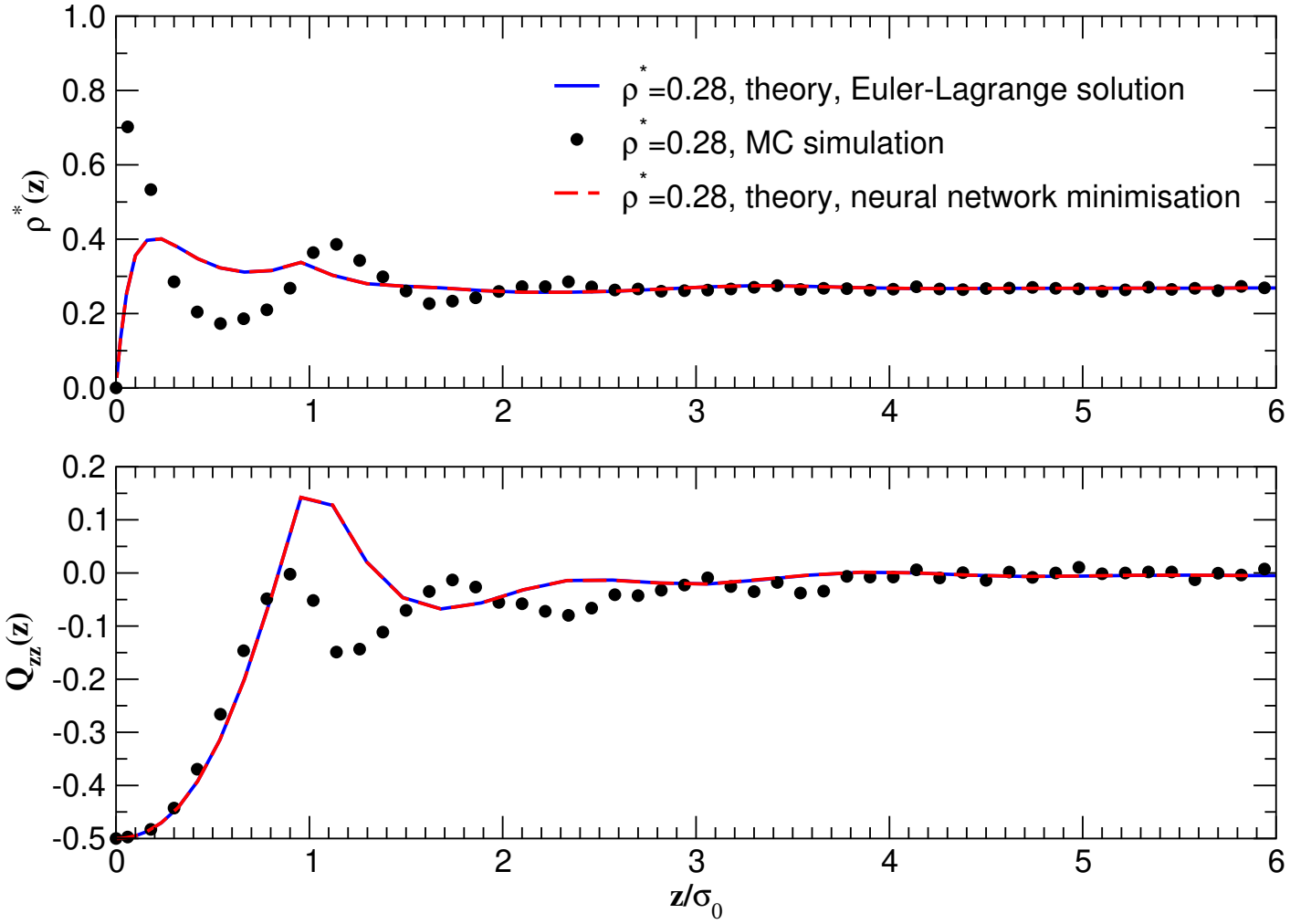

Results: density and Q profiles, symmetric film, $L_s = 2/3$

Bulk density $\rho^* = 0.35$ in N range

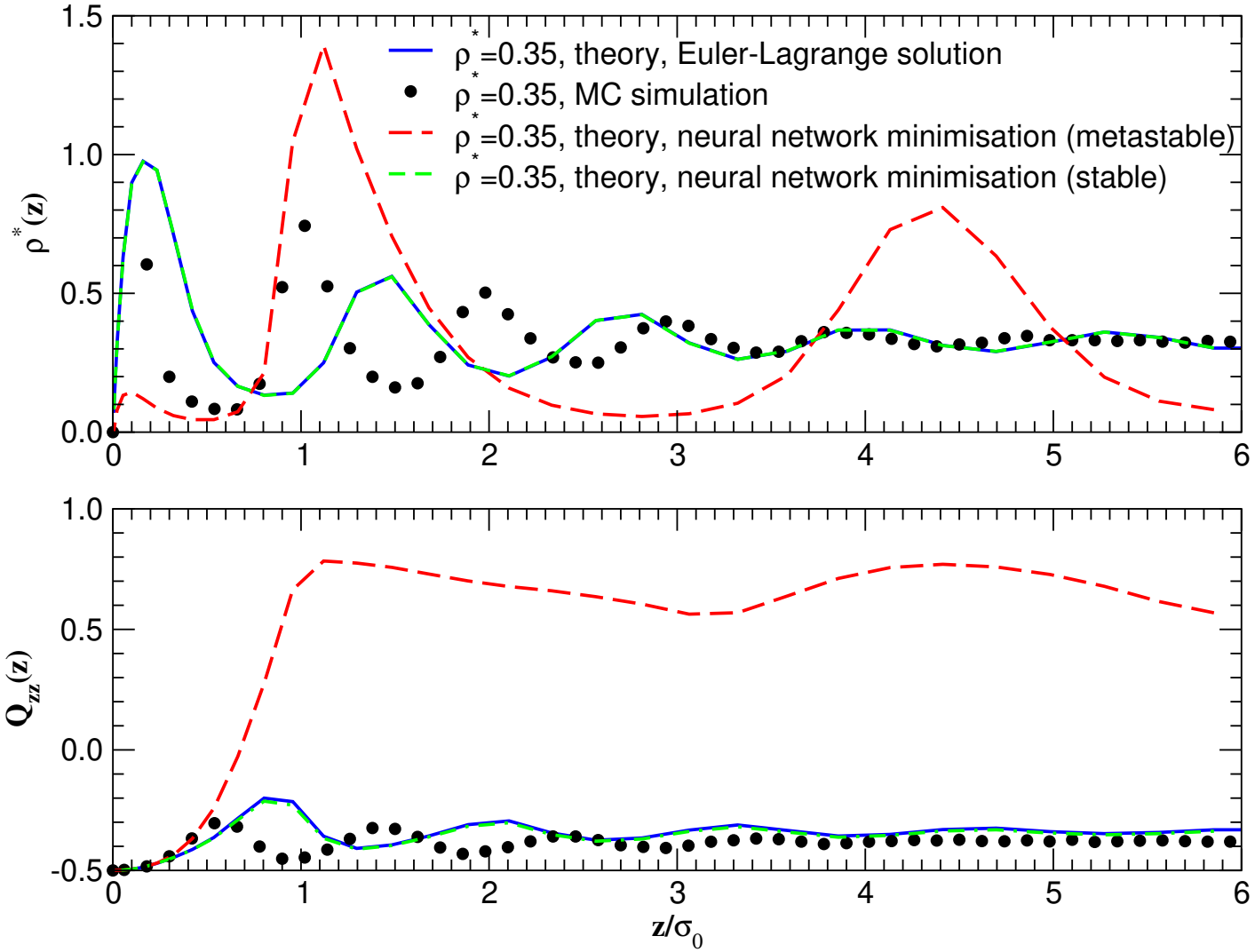

Results: density and Q profiles, hybrid film, variable L_z

Bulk density $\rho^* = 0.35$ in N range

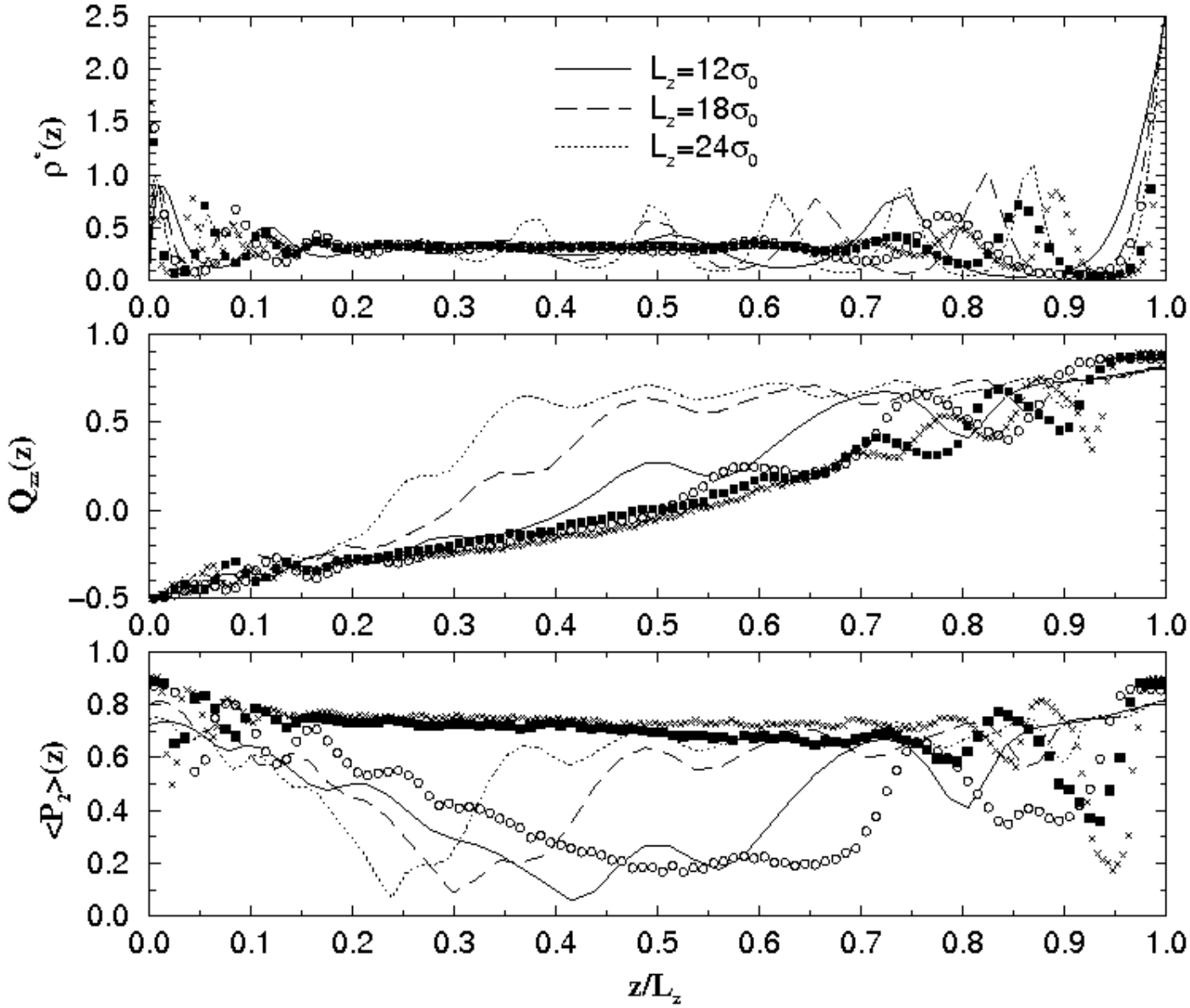

Results for discs

Simulations

- NVT Monte Carlo (MC), $N = 864$ particles.
- Bulk system: periodic boundary conditions. Ten different particle elongations, $\kappa = 0.05$, 0.1, 0.15, 0.2, 0.25, 0.3, 0.345, 0.35, 0.4 and 0.45, to find the phase diagram.
- Confined system: particles of $\kappa = 0.345$, sandwiched between two substrates a distance $L_z = 6\sigma_0$ apart. Periodic boundary conditions in transverse directions.
- Each system was compressed from the I phase into the N density range by increasing the number density by 0.1 after each run. At each density, run lengths of 10^6 MC sweeps (one sweep represents one attempted move per particle) were performed, averages being accumulated for the final 5×10^5 sweeps.

Results: density and Q profiles, symmetric film, $D_s = 1.0$

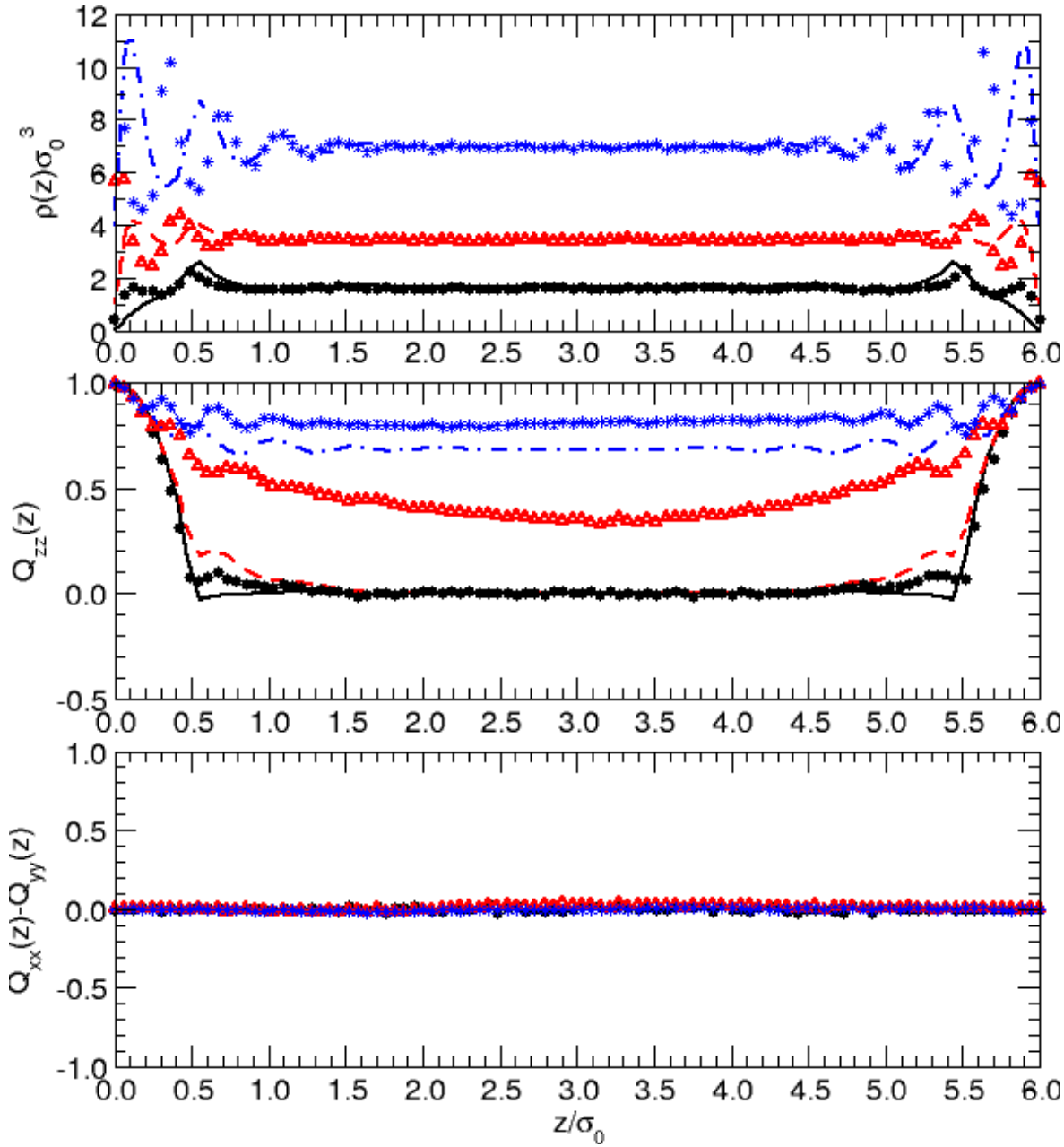

Results: density and Q profiles, symmetric film, $D_s = 0.0$

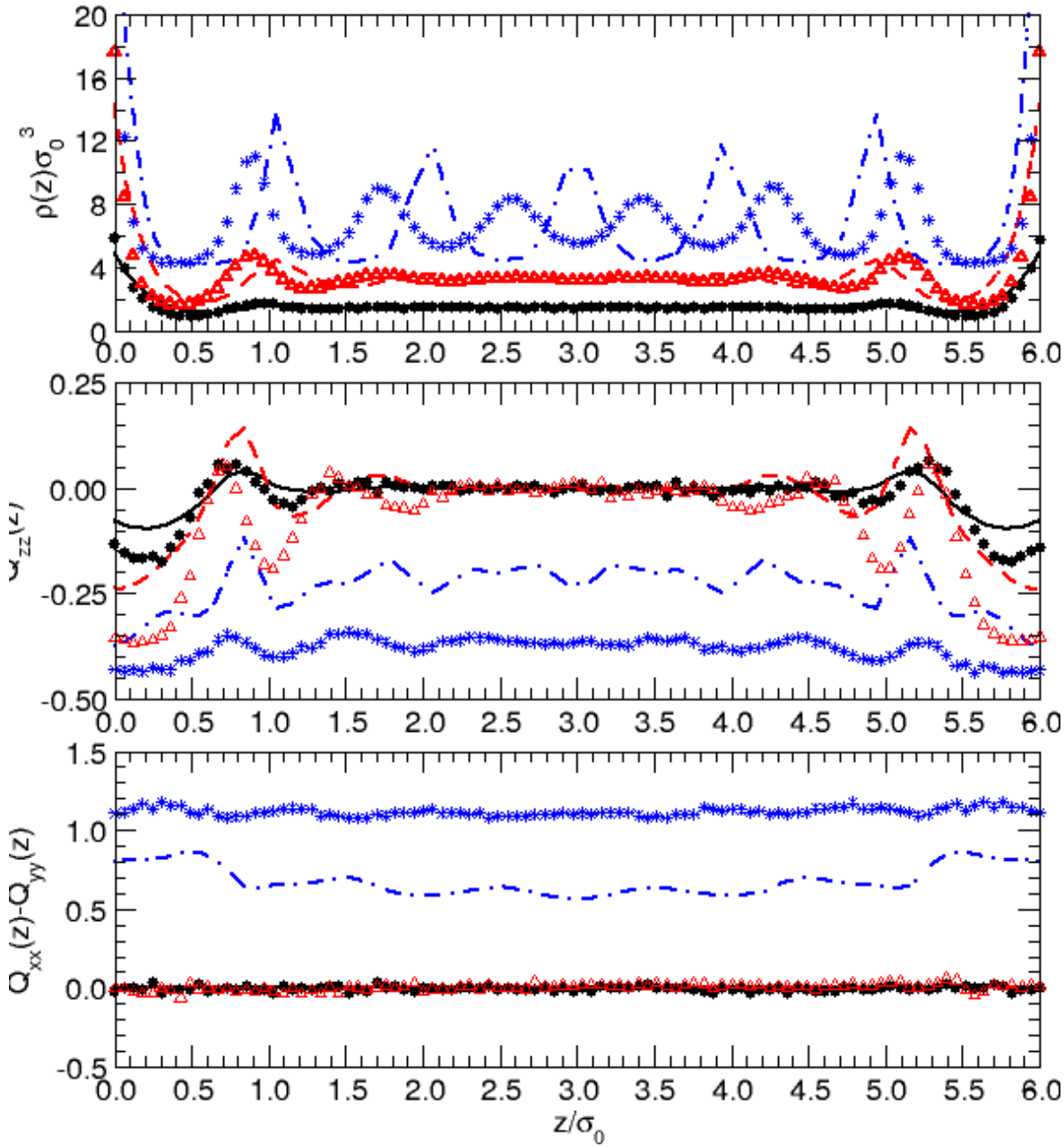

Results: density and Q profiles, symmetric film, $D_s = 0.5$

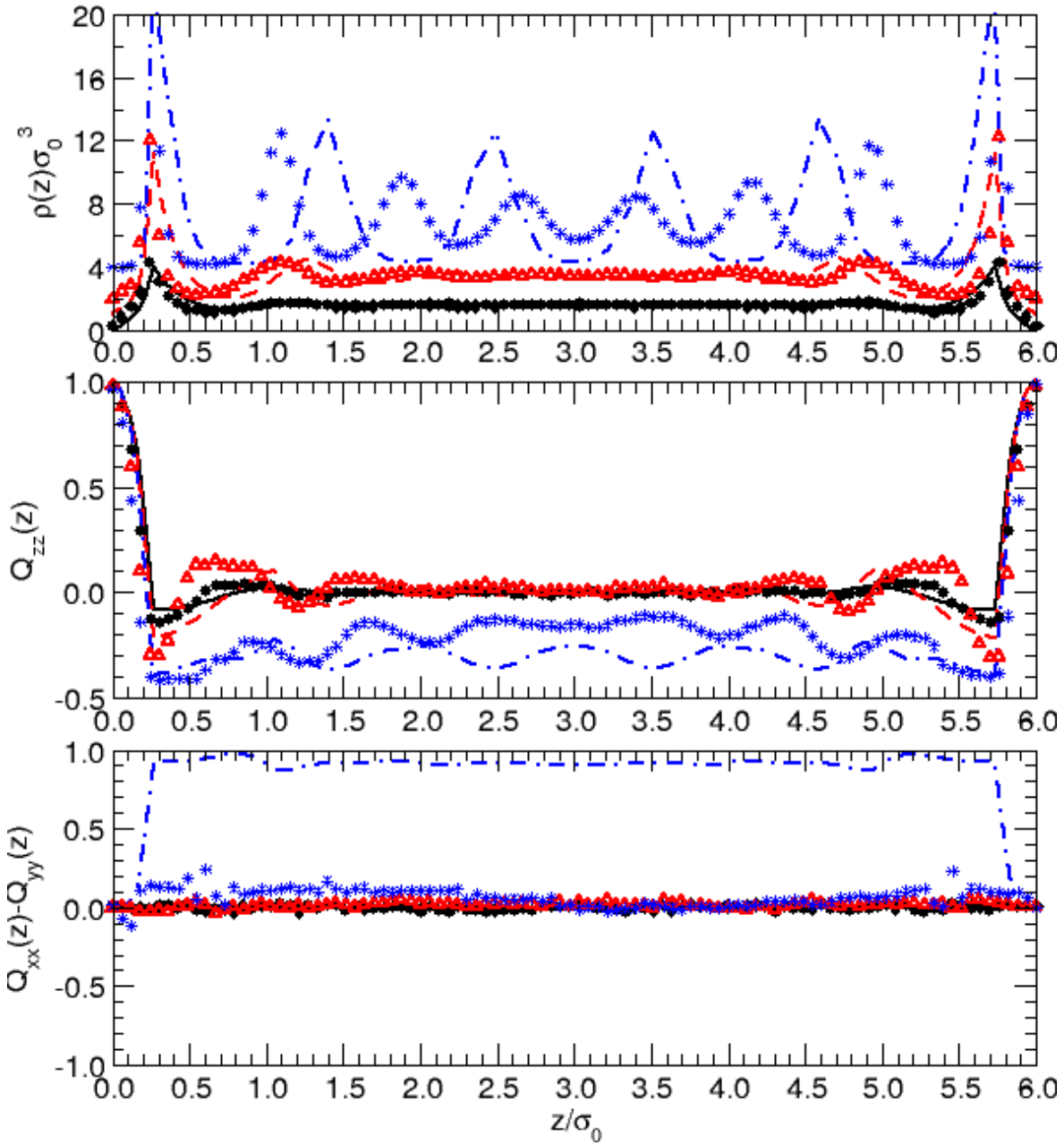

Results: density and Q profiles, symmetric film, $D_s = 0.55$

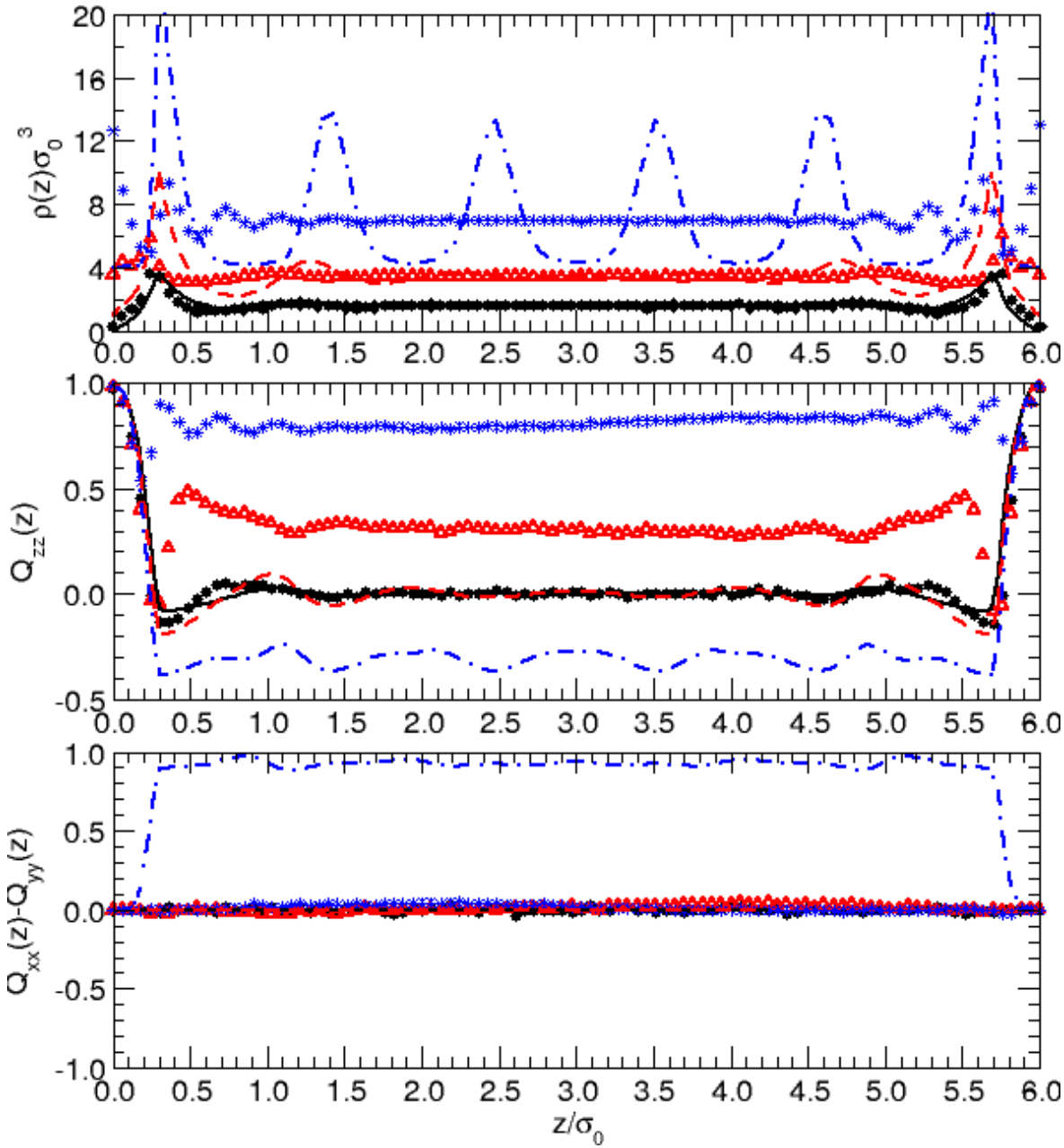

Results: density and Q profiles, symmetric film, $D_s = 0.7$

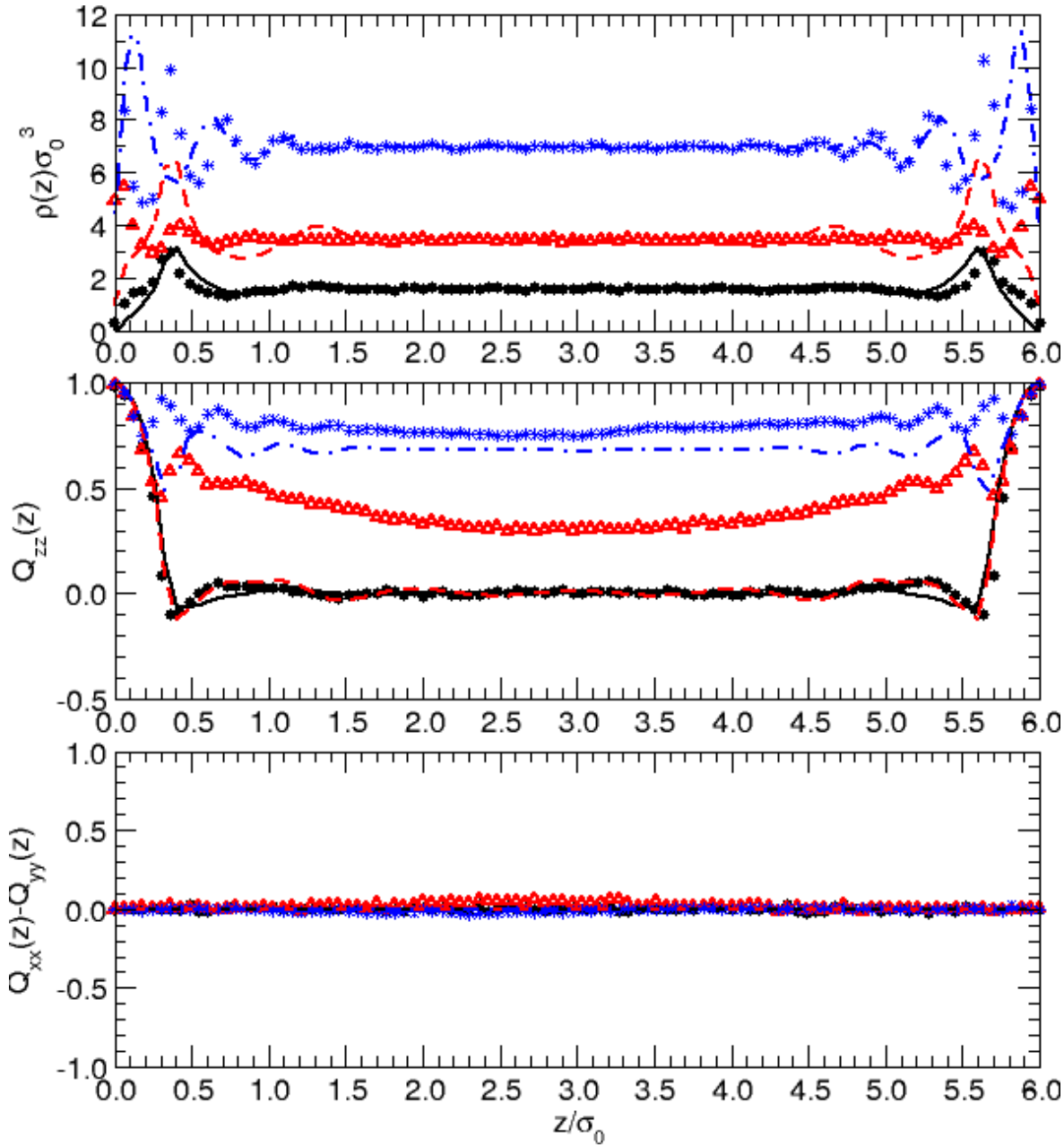

Results: configuration snapshots, symmetric film

$D_s = 0.0$

$D_s = 0.5$

$D_s = 0.55$

$D_s = 1.0$

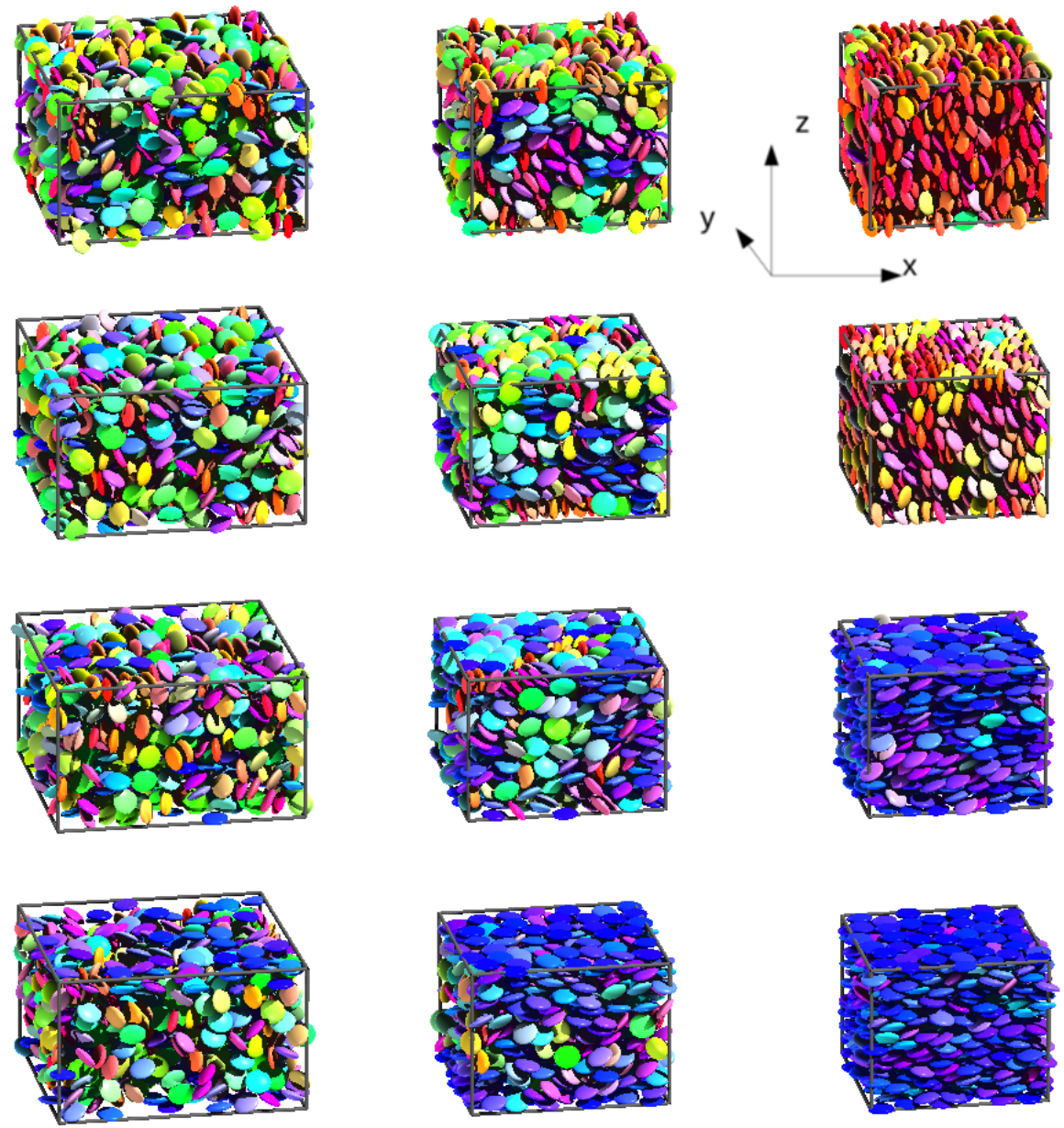

Results: spatially averaged q *vs* density, hybrid film

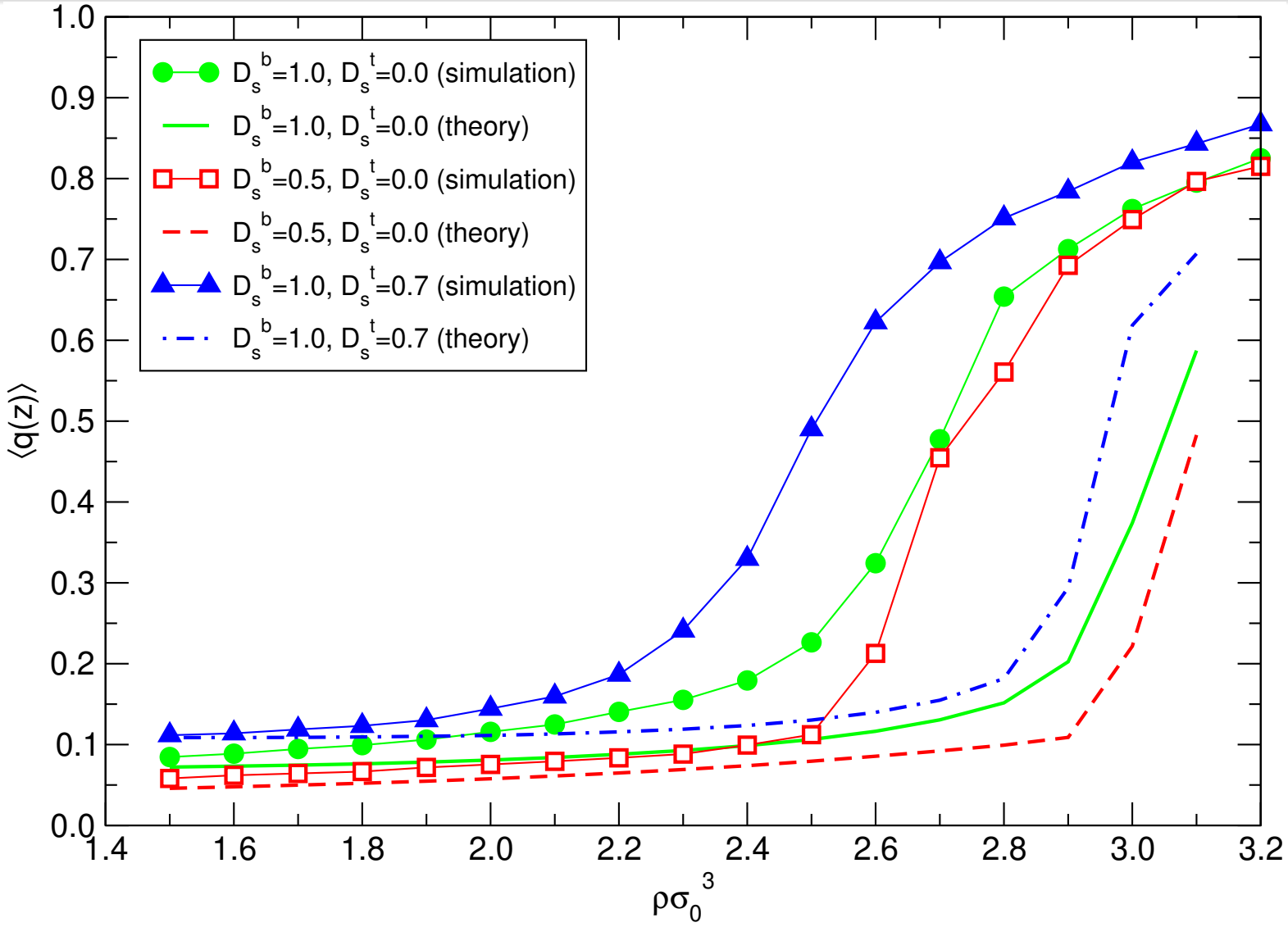

Both theory and simulation yield a continuous variation, Theory overestimates the density of the para-N–N transition. Homeotropic films order more easily than planar ones.

Results: spatially averaged $Q_{xx} - Q_{yy}$ *vs* density, hybrid film

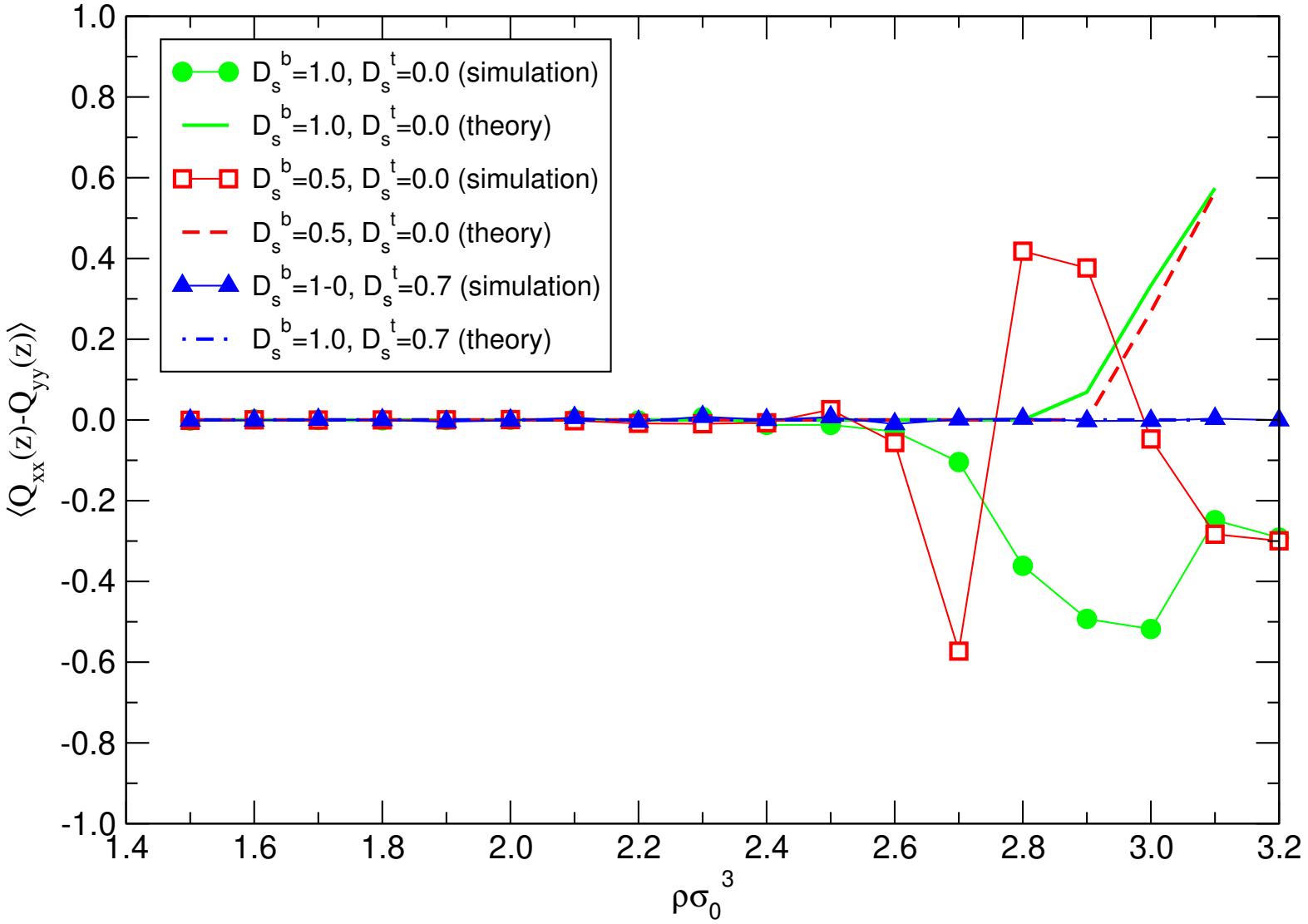

Theory and simulation agree there is some biaxiality, except when anchoring is uniform homeotropic (face-on) throughout the film.

Results: density profiles, hybrid film, $D_s^b = 1.0$, $D_s^t = 0.0$

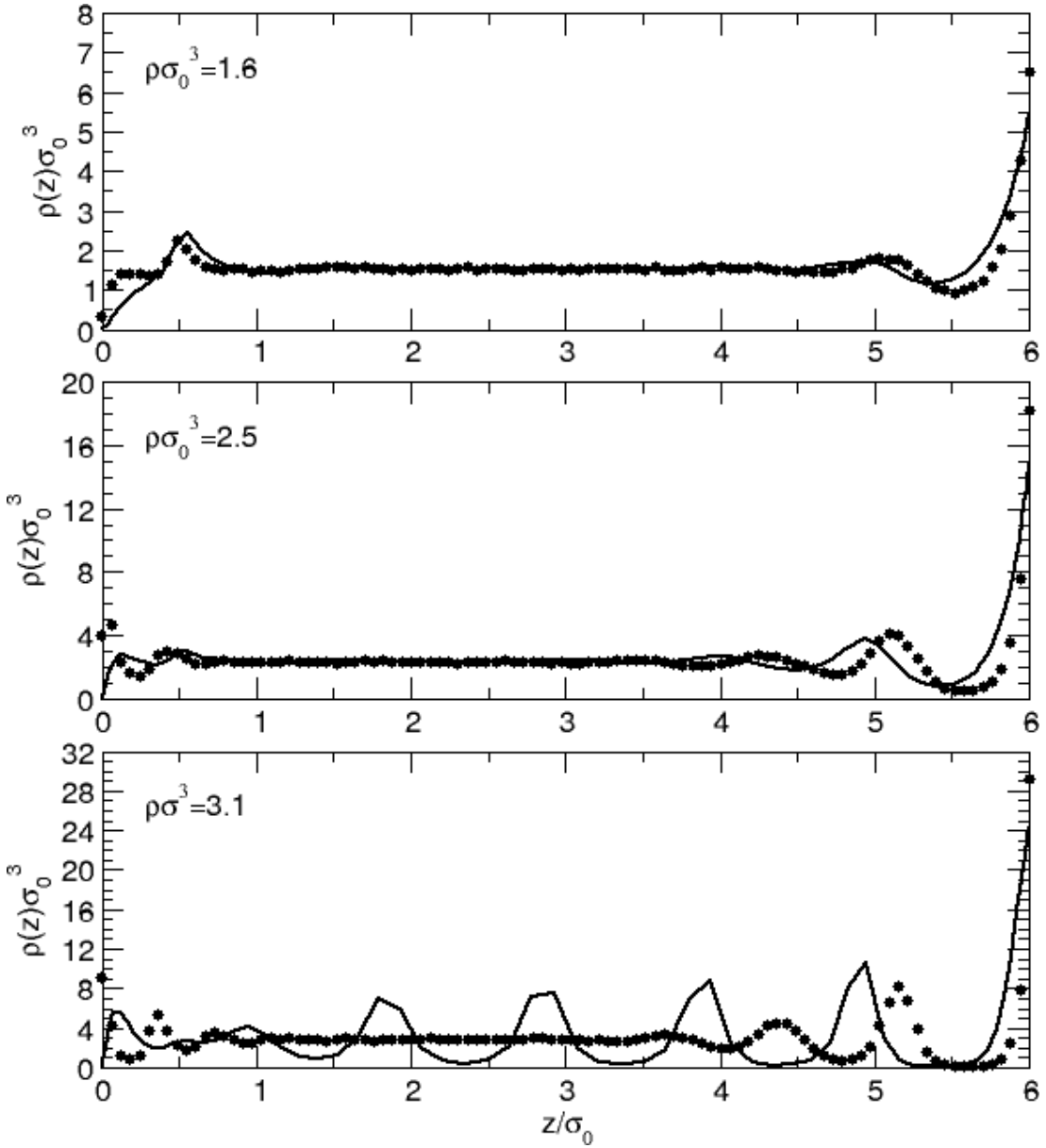

Results: Q profiles, hybrid film, $D_s^b = 1.0$, $D_s^t = 0.0$

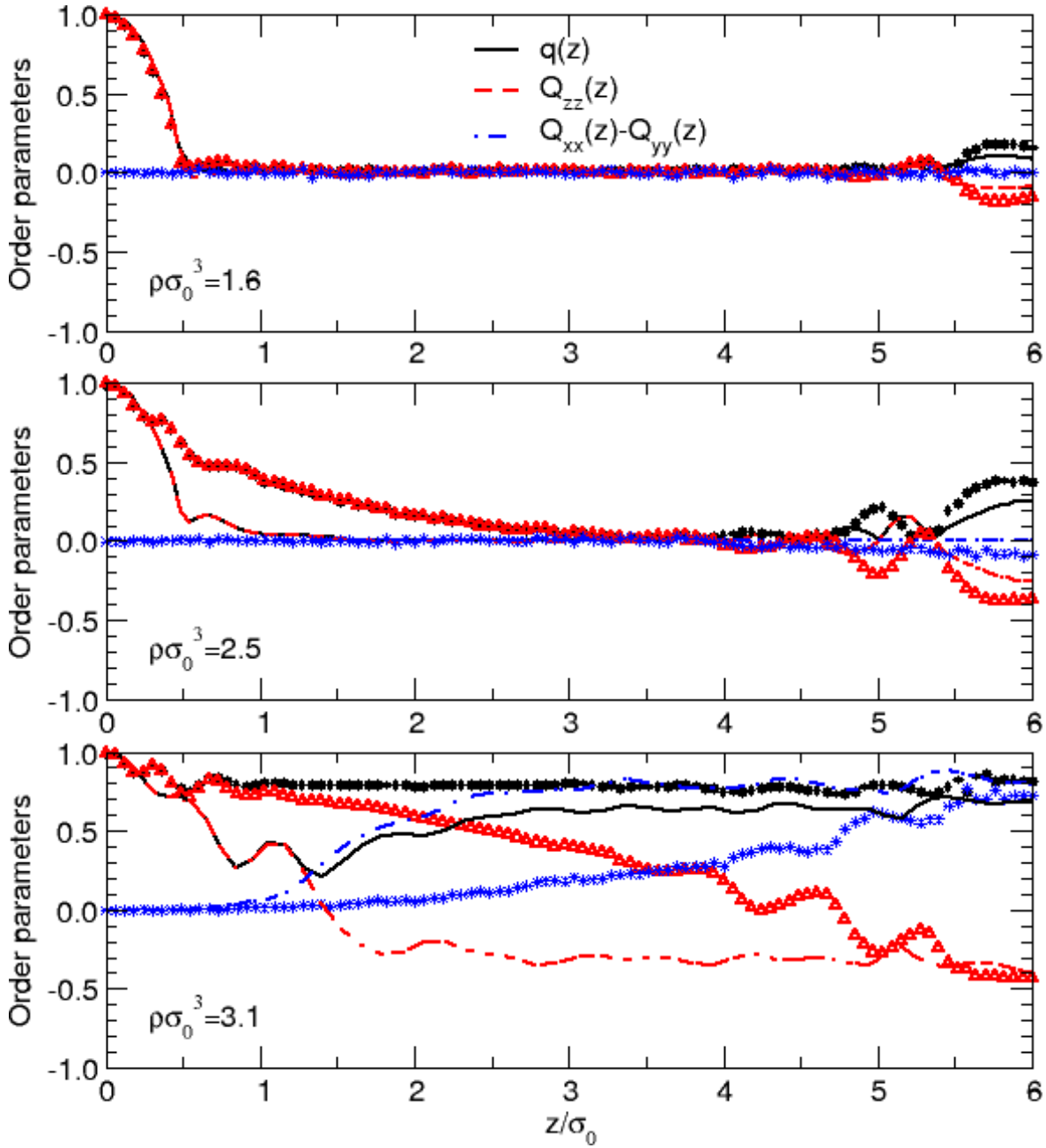

Results: density profiles, hybrid film, $D_s^b = 1.0$, $D_s^t = 0.7$

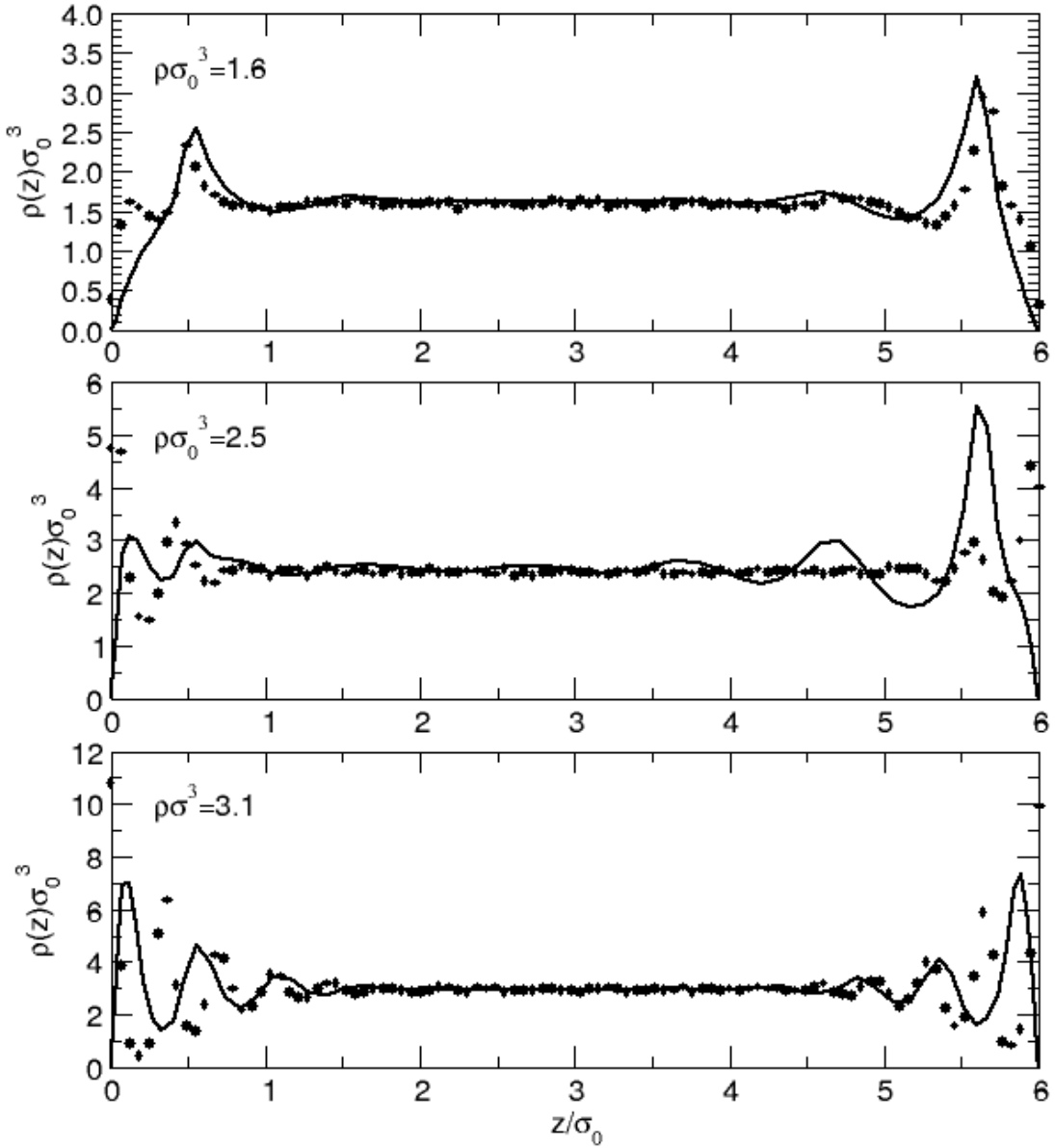

Results: Q profiles, hybrid film, $D_s^b = 1.0$, $D_s^t = 0.7$

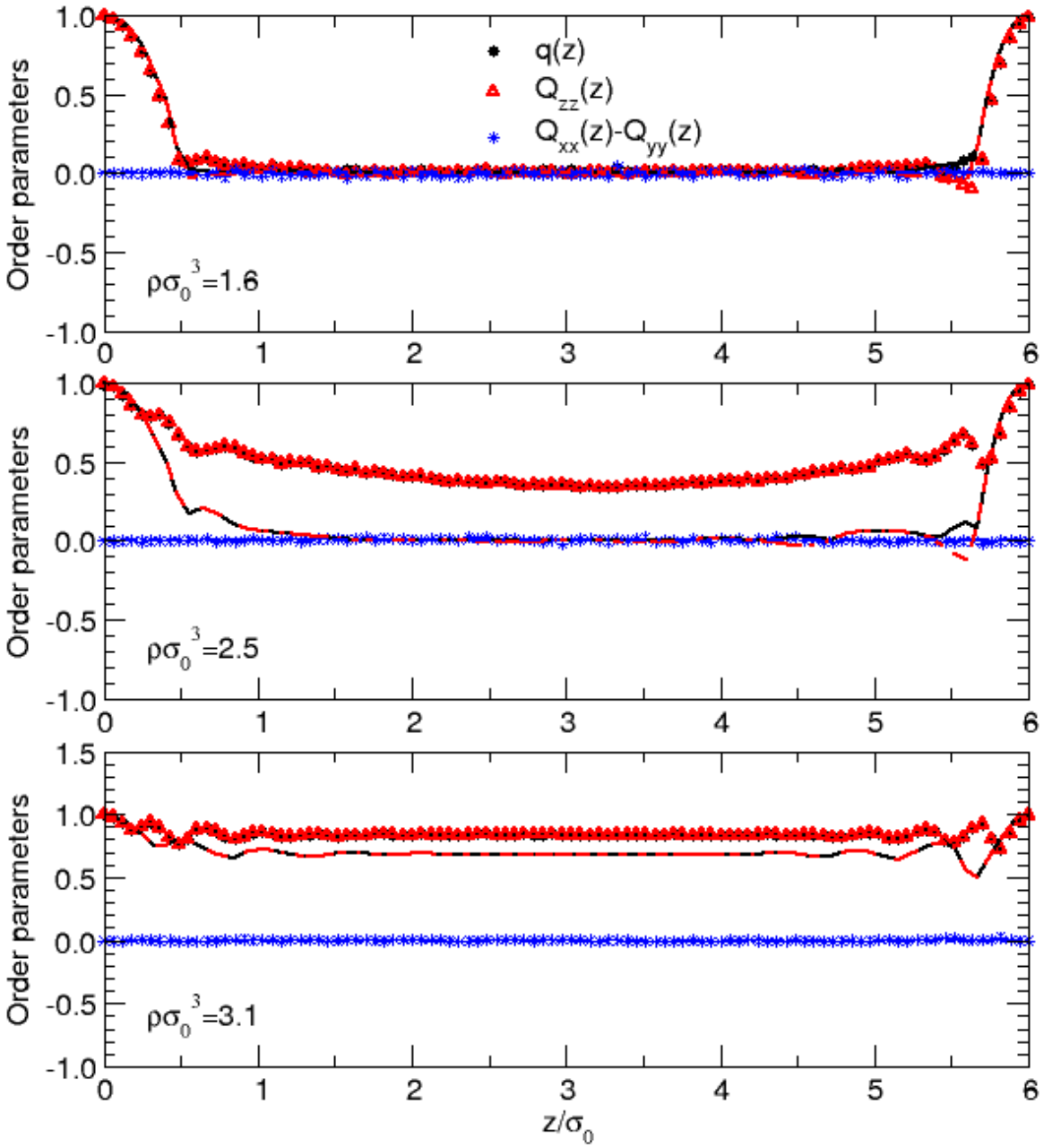

Results: density profiles, hybrid film, $D_s^b = 0.5$, $D_s^t = 0.0$

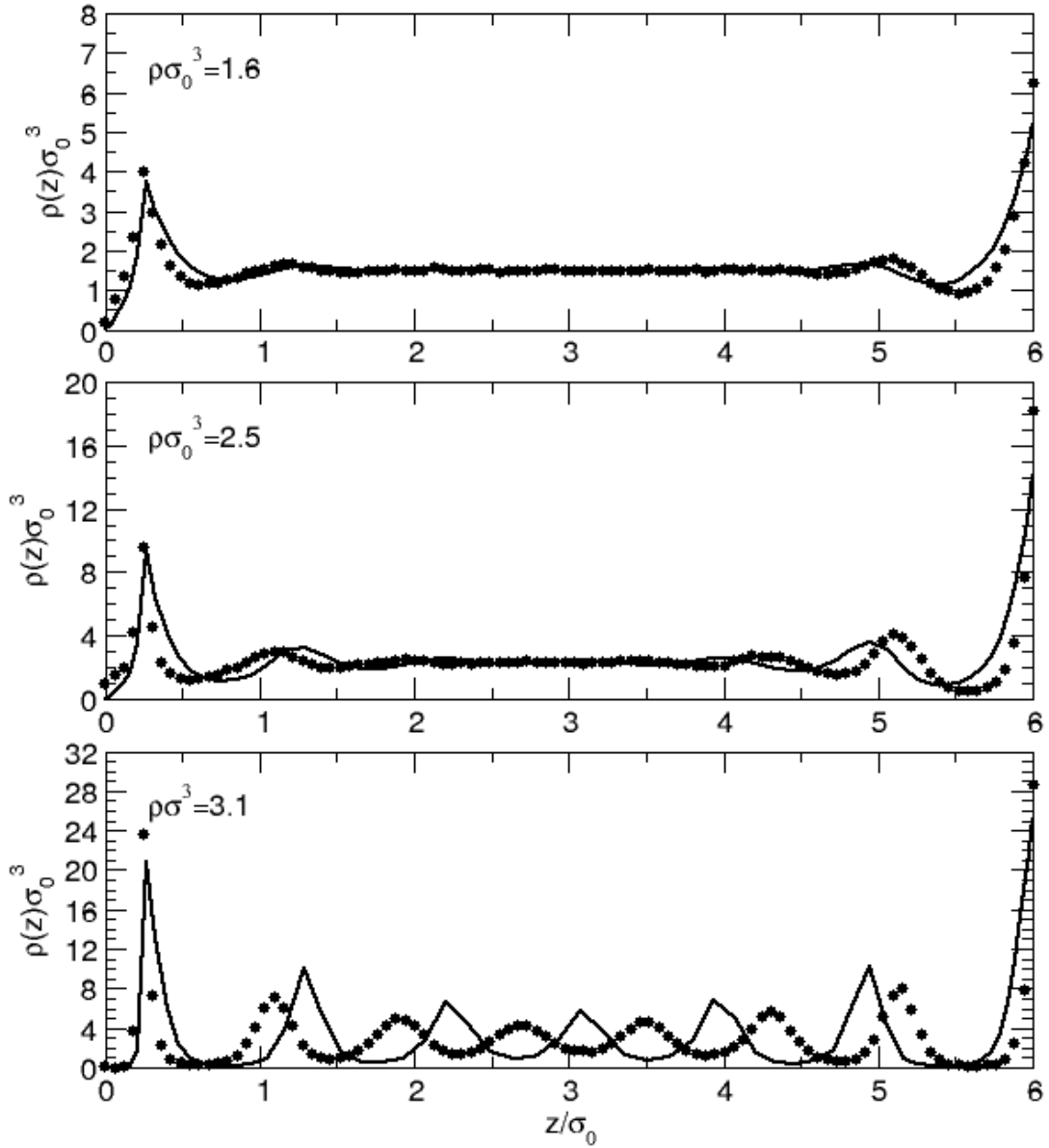

Results: Q profiles, hybrid film, $D_s^b = 0.5$, $D_s^t = 0.0$

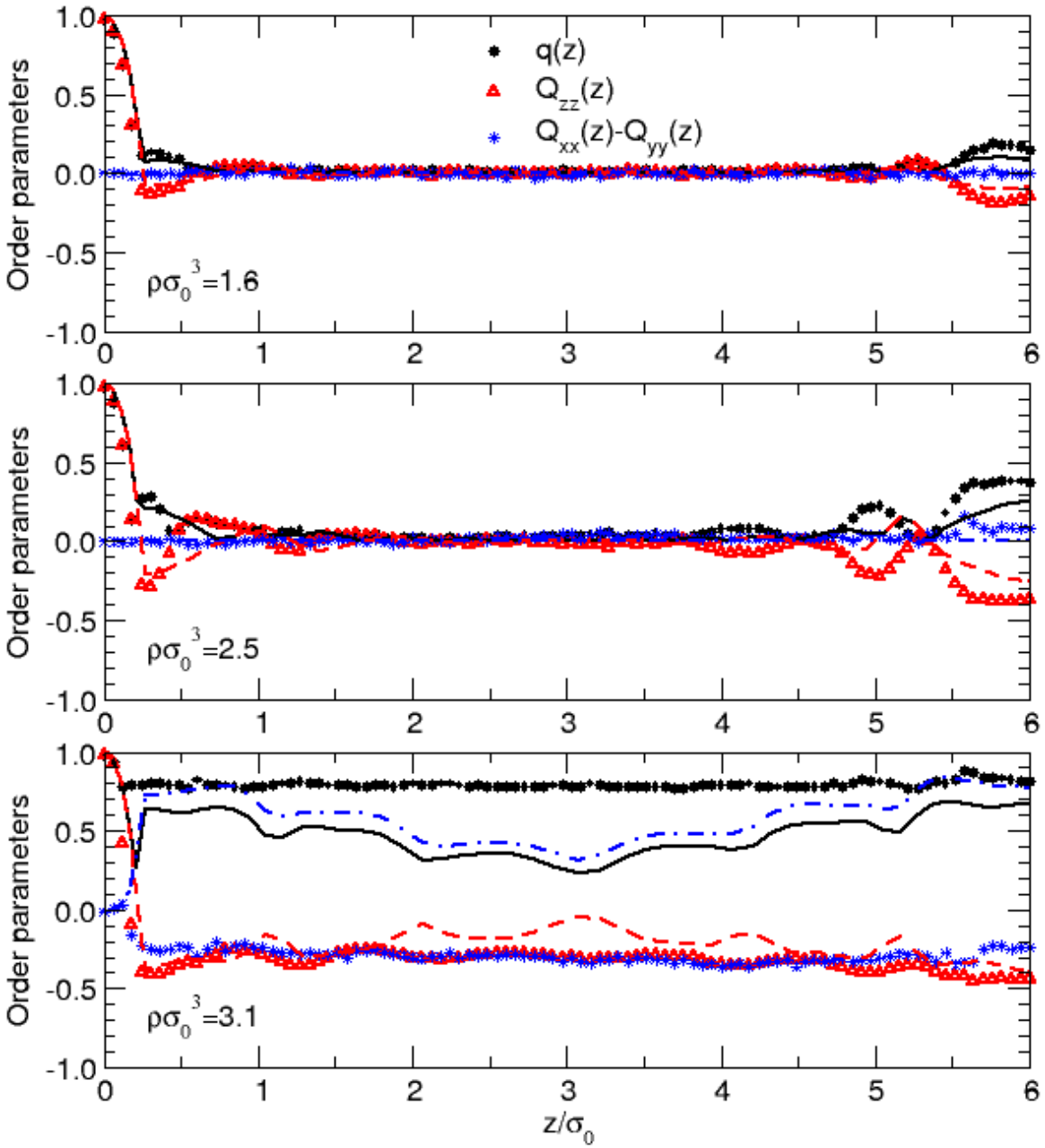

Results: regime diagram from simulation, hybrid film

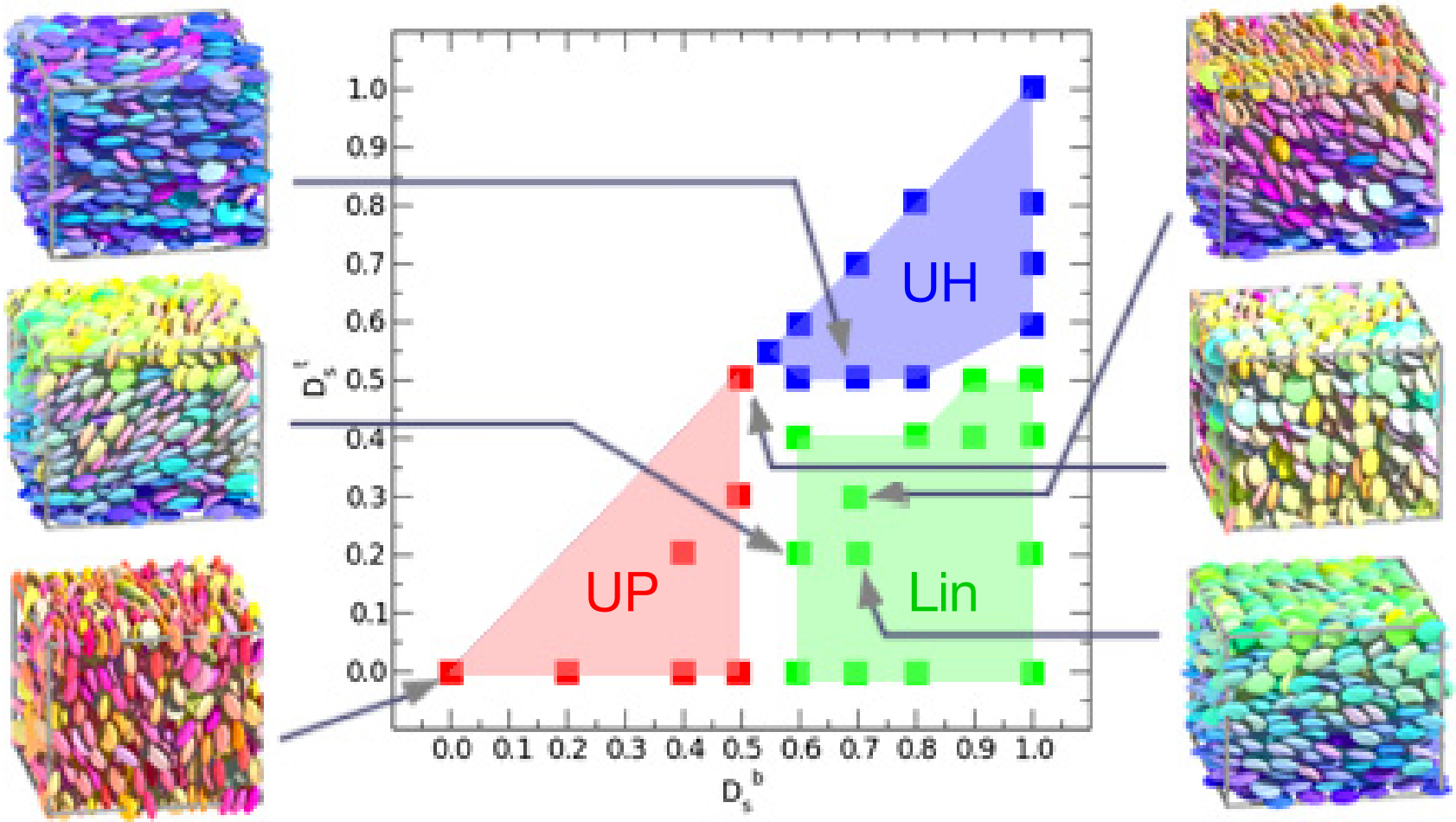

Results: configuration snapshots, hybrid film

$D_s^b = 1.0,\ D_s^t = 0.0$

$D_s^b = 1.0,\ D_s^t = 0.7$

$D_s^b = 0.5,\ D_s^t = 0.0$

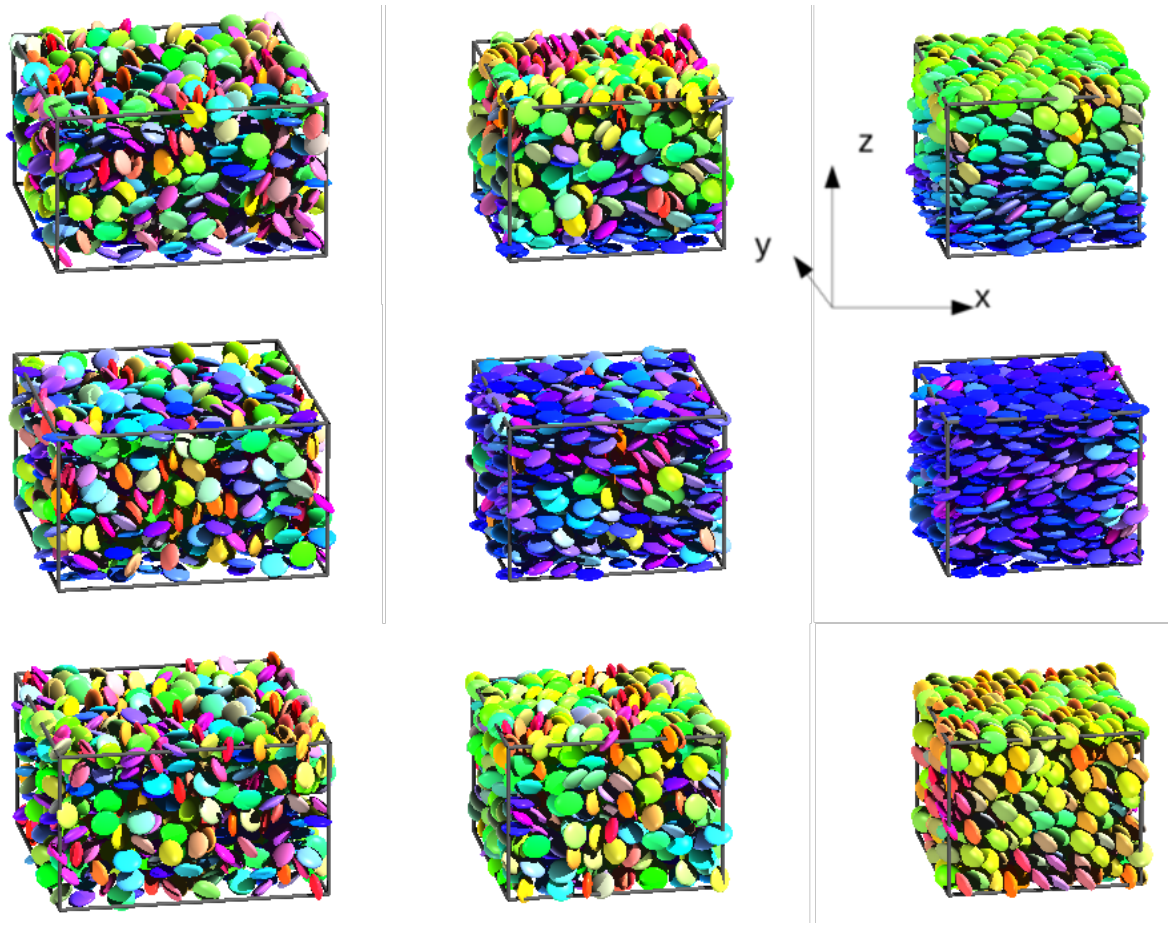

Conclusions

- We have proposed a very simple microscopic model for both rod-like and disc-like liquid crystals sandwiched between boundaries of variable penetrability.
- This model, coupled with density-funcional formalism, provides molecular-level control over surface anchoring properties.
- The simple Onsager approximation of DFT, combined with Parsons-Lee density re-scaling, can be useful for describing the structure of fluids of prolate or oblate HGO particles of moderate elongation confined between two penetrable walls/large particles.
- Although our theory is qualitatively reliable, quantitatively it performs rather more poorly for oblate than for prolate paticles. Expected to improve for thicker films, this work is in progress.
- We are currently working on implementing more accurate approximations.
- Use of minimisation NNs appears promising (reliable + cheap + fast).

Acknowledgements

We acknowledge funding from the following sources:

- British Council, Treaty of Windsor Grant No. B-54/07.
- Engineering and Physical Research Council (UK), Grant No. GR/S59833/01.
- Fundação para a Ciência e Tecnologia (Portugal), Contracts and Grants Nos.
  - PTDC/FIS/098254/2008
  - PEst-OE/FIS/UI0618/2011
  - EXCL/FIS-NAN/0083/2012
  - UIDB/00618/2020
  - UIDP/00618/2020
- Instituto Politécnico de Lisboa (IPL), Project IPL/2019/DISCONEDGE_ISEL

Shameless publicity plug

Topics

- Liquid Crystals in Biology and Active Matter
- Macromolecular Liquid Crystals
- Confined Liquid Crystals
- Design of New Materials
- Mathematical Modelling, Symmetry and Topology
- Novel Applications

How we find the phase diagram from *NVT* MC simulation

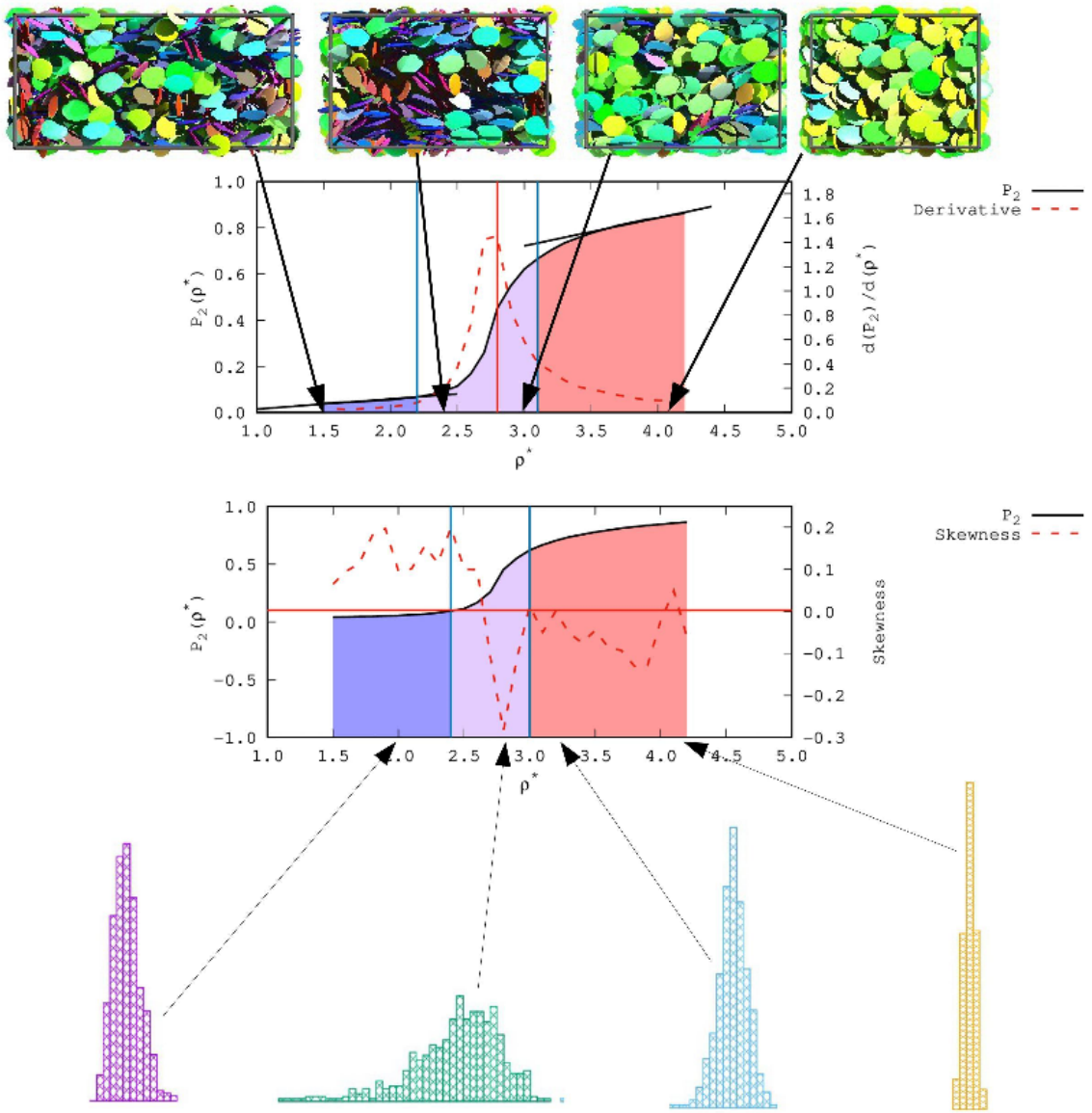

Results: bulk order parameter *vs* density

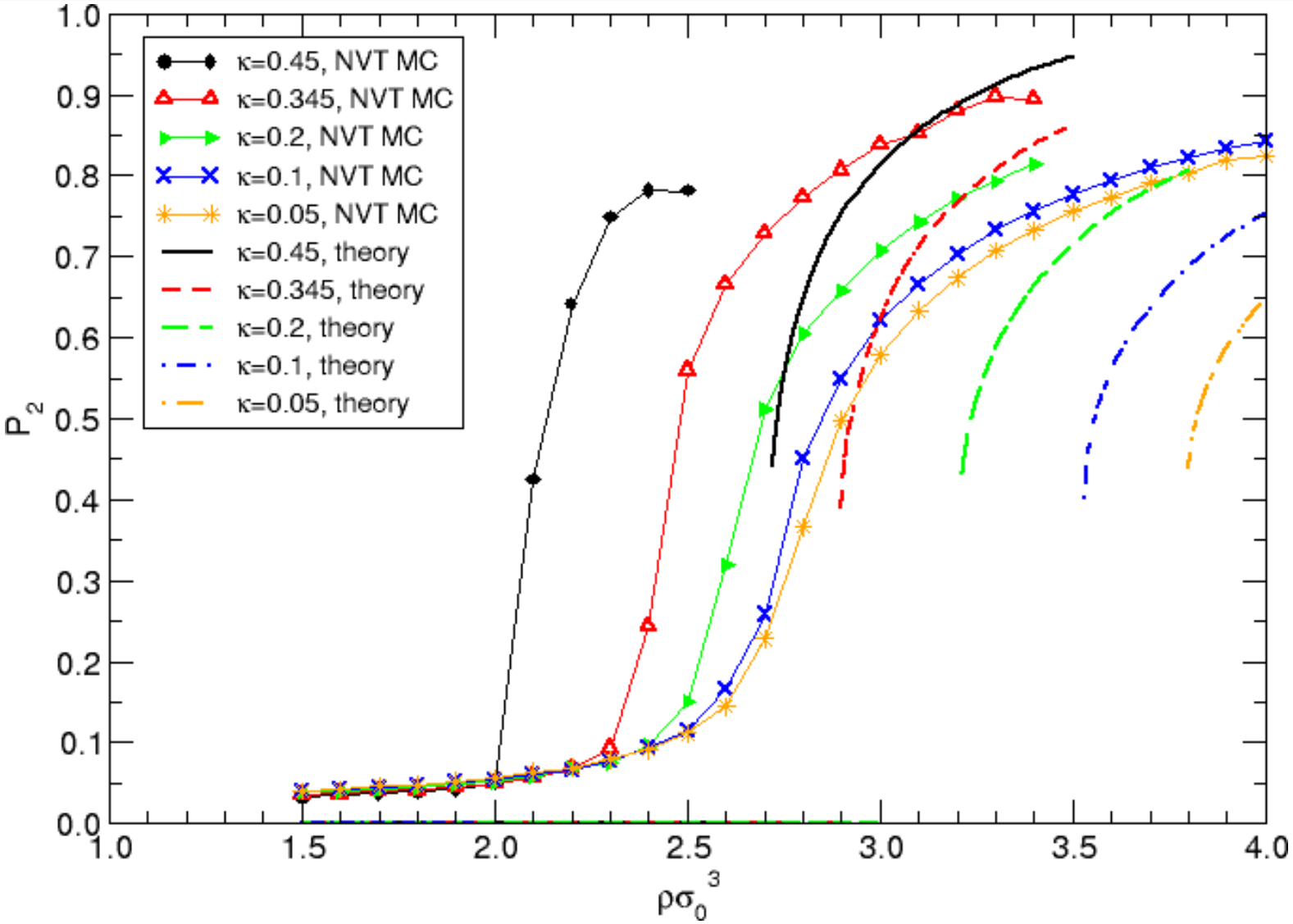

Simulation results show a continuous variation, whereas theory predicts a jump at the (first-order) I–N transition.